



Effects of soluble guanylate cyclase activator vericiguat on fracture healing in rats

Azat Dzhumukov, MD¹, Bilal Karabak, MD², Aziz Demirci, MD², Ferhat Yıldırım Hoyur, MD³,
Muhammed Çağatay Engin, MD⁴

¹Department of Orthopedics and Traumatology, Torbalı State Hospital, İzmir, Türkiye

²Department of Orthopedics and Traumatology, Erzurum City Hospital, Erzurum, Türkiye

³Department of Orthopedics and Traumatology, Yavuz Selim Bone Disease and Rehabilitation Hospital, Trabzon, Türkiye

⁴Department of Orthopedics and Traumatology, Atatürk University Hospital, Erzurum, Türkiye

Bone restoration to its original form and operational state without scar tissue formation defines the biological process of fracture healing. The healing process of fractures starts immediately after injury and requires the coordinated action of multiple molecular elements and cellular components and biomechanical factors.^[1] It has been reported that 5 to 10% of fractures occurring annually in the United States experience healing problems of varying degrees.^[2] The failure of fractures to heal properly requires additional medical procedures and repeated surgeries and extended work disability and substantial financial expenses.

The underlying causes of these complications include multifactorial etiology such as age, nutritional status, hormonal changes, inadequate

Received: September 25, 2025

Accepted: November 29, 2025

Published online: March 16, 2026

Correspondence: Muhammed Çağatay Engin, MD. Atatürk Üniversitesi Hastanesi, Ortopedi ve Travmatoloji Kliniği, 25040 Yakutiye, Erzurum, Türkiye.

E-mail: azat.dzhumukov@gmail.com

Doi: 10.52312/jdrs.2026.2655

Citation: Dzhumukov A, Karabak B, Demirci A, Hoyur FY, Engin MÇ. Effects of soluble guanylate cyclase activator vericiguat on fracture healing in rats. Jt Dis Relat Surg 2026;37(2):519-530. doi: 10.52312/jdrs.2026.2655.

© 2026 Joint Diseases and Related Surgery. This is an open access article published under the terms of the Creative Commons Attribution-NonCommercial 4.0 International License (CC BY-NC 4.0), which permits non-commercial use, distribution, reproduction, and adaptation in any medium, provided the original work is properly cited. <http://creativecommons.org/licenses/by-nc/4.0/>

ABSTRACT

Objectives: The aim of this study was to assess the healing effects of vericiguat at various concentrations on rat femur fractures through clinical and radiological and biomechanical and histopathological assessments.

Materials and methods: In this study, a total of 60 female Wistar-Albino rats were used. The study comprised of six rat groups with 10 rats in each group: Group 1 (normal controls), Group 2 (positive controls - only fracture), Group 3 (low-dose vericiguat - 3 mg/kg), Group 4 (high-dose vericiguat - 6 mg/kg), Group 5 (fracture + low-dose vericiguat), Group 6 (fracture + high-dose vericiguat). Under general anesthesia, standard closed fractures were created in the right femurs of rats in the fracture groups. Radiological examinations were performed on Days 7, 14, and 28. The Lane-Sandhu scoring system was used for radiological assessment. At the end of Day 28, the rats were sacrificed, and the fracture healing tissues were examined biomechanically and histologically using the Huo scale.

Results: The 28th day biomechanical assessment showed significant differences in maximum load values between the fractured groups (Group 2: 88.75 ± 23.25 N, Group 5: 83.54 ± 23.15 N, Group 6: 39.07 ± 10.38 N; $p = 0.003$). The stiffness values showed similar patterns (Group 2: 64.71 ± 45.52 N/mm, Group 5: 99.20 ± 43.82 N/mm, Group 6: 40.47 ± 19.27 N/mm; $p = 0.088$). In the histological evaluation according to the Huo scale, Group 5 showed the highest quality of healing (8.6 ± 1.14) and a significant difference was found between Group 2 and Group 5 ($p = 0.009$). Group 6 demonstrated necrosis in four out of 10 animals and severe inflammation in eight out of 10 animals. In the radiological evaluation on Days 7, 14, and 28, no statistically significant differences were observed between the groups according to the Lane-Sandhu scoring system ($p = 0.811$ on Day 14; $p = 0.299$ on Day 28).

Conclusion: Our study results suggest that soluble guanylate cyclase (sGC) activators show promise for fracture healing treatment when used at specific concentrations, but their therapeutic range remains limited and their toxic effects at high doses need careful consideration.

Keywords: Fracture healing, guanylate cyclase, rats, vericiguat.

reduction, concomitant diseases, infections, medications used, and the characteristics of the trauma.^[3] Recent advances in the study of bone metabolism signalling pathways have revealed novel therapeutic targets.

The research community currently focuses on guanylate cyclase because this enzyme produces cyclic guanosine monophosphate (cGMP) while controlling vital cellular processes including signal transduction and gene expression and cell movement.^[4,5] Research has established sGC as a new therapeutic target for bone diseases, as sGC activation produces positive effects for osteoporosis management.^[4] Several studies have demonstrated that guanylate cyclase activation produces dual effects on osteoclast differentiation at the bone tissue level.^[6] The increase of guanylate cyclase activity through mechanical stimulation leads to osteoblast proliferation.^[7]

Vericiguat is a new-generation oral activator of soluble guanylate cyclase (sGC) which has established itself in cardiovascular medicine. The clinical evidence from 2020 demonstrated its ability to decrease cardiovascular death rates and hospital admissions among heart failure patients.^[8] The mechanism of action of vericiguat is based on the activation of the nitric oxide (NO)-soluble guanylate cyclase-cGMP signaling pathway through direct cGMP production. Research using molecular techniques demonstrates that vericiguat controls osteoclast development and bone destruction by affecting vasodilator-stimulated phosphoprotein (VASP) and nuclear factor kappa-light-chain-enhancer of activated B cells (NF- κ B) signaling pathways.^[6] This signaling pathway is known to play critical roles in bone metabolism and remodeling processes.^[4] The study employed two dose levels (3 mg/kg and 6 mg/kg) to investigate the therapeutic window and potential toxicity threshold of vericiguat in bone healing.

While there are limited studies on sGC activators' effects on bone tissue, previous animal models using sGC agonists have shown both beneficial and adverse effects on bone remodeling depending on dosage.^[4,8] There are no experimental studies specifically investigating the direct effects of vericiguat on fracture healing processes. The current understanding suggests that vericiguat may influence fracture healing, as it affects signaling pathways which control bone metabolism.

In the present study, we, for the first time, aimed to assess the healing effects of vericiguat

at various concentrations on rat femur fractures through clinical and radiological and biomechanical and histopathological assessments.

MATERIALS AND METHODS

This randomized-controlled experimental study was conducted in accordance with the ARRIVE guidelines 2.0 for reporting animal research.^[9] The study protocol was approved by the Atatürk University Animal Experiments Ethics Committee (Date: 05.05.2023, No: E-42190979-000-2300144669).

Using 80% study power and 5% alpha error, the sample size was calculated for biomechanical load testing with $d = 0.8$ effect size and 15 N standard deviation (SD) which required 10 animals per group. Between May 2023 and October 2023, a total of 60 Wistar-Albino female rats were distributed across 10 subjects per group. The study included female rats aged 2.7 to 2.9 months weighing between 150 to 280 g who maintained good health status. The exclusive use of female rats was chosen to reduce experimental variability; however, estrous cycle variations were not controlled. The study excluded rats that were pregnant or had previous surgical procedures or showed signs of infection or abnormal movement disorders or had general health conditions that made anesthesia unsafe. Vericiguat (Verquvo® 10-mg film-coated tablet; Bayer AG, Leverkusen, Germany) was dissolved in 0.5% methylcellulose solution as vehicle. Control groups received equivalent volumes of vehicle alone. The study defined vericiguat administration as an oral gavage administration of 3 mg/kg/day (low dose) and 6 mg/kg/day (high dose) based on the animal body weights. The researchers chose these specific doses, since previous research showed that bone metabolism responded differently to various dose levels.^[4,10]

Study procedures

Standardized methods enabled the research team to conduct radiological assessments on Days 7, 14, and 28 and to perform biomechanical and histopathological assessments on Day 28. The researchers established biomechanical load capacity on Day 28 as their primary outcome measure. The study evaluated three secondary outcomes through Lane-Sandhu radiological healing scores^[11] and Huo scale^[12] histological healing scores and complication rates. According to the laboratory protocol, the animals were housed under standard laboratory conditions at 22°C, 50 ± 5% humidity, and a 12-h light/dark cycle. The anesthesia protocol

required intraperitoneal administration of ketamine (Ketasol 10% Richter Pharma AG, Wels, Austria) at 52 mg/kg combined with xylazine (Rompun 2%, Bayer AG, Leverkusen, Germany) at 8 mg/kg. The veterinary team administered subcutaneous carprofen at 5 mg/kg for three days to provide post animal distress. Animals that developed surgical site infections, experienced Kirschner wire (K-wire) migration, or died unexpectedly during the study were excluded from the analysis. The researchers checked animals every day to detect any signs of infection or implant failure or during the follow-up period. The follow-up protocol included both daily clinical observations and weekly weight measurements together with radiological examinations at specific time points. Radiological evaluations using the Lane-Sandhu scoring system maintained their reliability through blind assessment by three orthopedic specialists who achieved an inter-observer reliability coefficient of 0.85. Standardized test parameters along with INSTRON 5982 (Instron Corp., Norwood, MA, USA) device calibration validated the biomechanical tests. The Huo scale served as the method to evaluate histological samples through a 1-10 maturity system which shows bone union development from fibrous tissue to fully formed bone.^[12] All histological

assessments were performed by two blinded observers independently.

Intervention protocol and surgical method

The subjects received random assignment to six groups consisting of Group 1 (NC) with healthy controls (n = 10) and Group 2 (PC) with fracture + K-wire controls (n = 10) and Group 3 (LDV-N) with low-dose vericiguat (n = 10) and Group 4 (HDV-N) with high-dose vericiguat (n = 10) and Group 5 (LDV-P) with fracture + K-wire + low-dose vericiguat (n = 10) and Group 6 (HDV-P) with fracture + K-wire + high-dose vericiguat (n = 10). The researchers used the sealed envelope method for randomization with allocation concealment. Treatment solutions were coded as A, B, and C by an independent researcher to ensure blinding of the intervention. Investigators performing assessments remained unaware of group allocation throughout the study. A 1-cm incision was made in the anterior region of the right knee to expose the femoral condyles (Figure 1a), an intramedullary entry hole was prepared (Figure 1b), and a K-wire (1.0 mm in diameter, Zimmer Biomet, Warsaw, IN, USA) was inserted (Figure 1c). The fracture was created using controlled three-point bending with a standardized force of 20 N applied perpendicular to the femoral shaft (Figure 1d) to

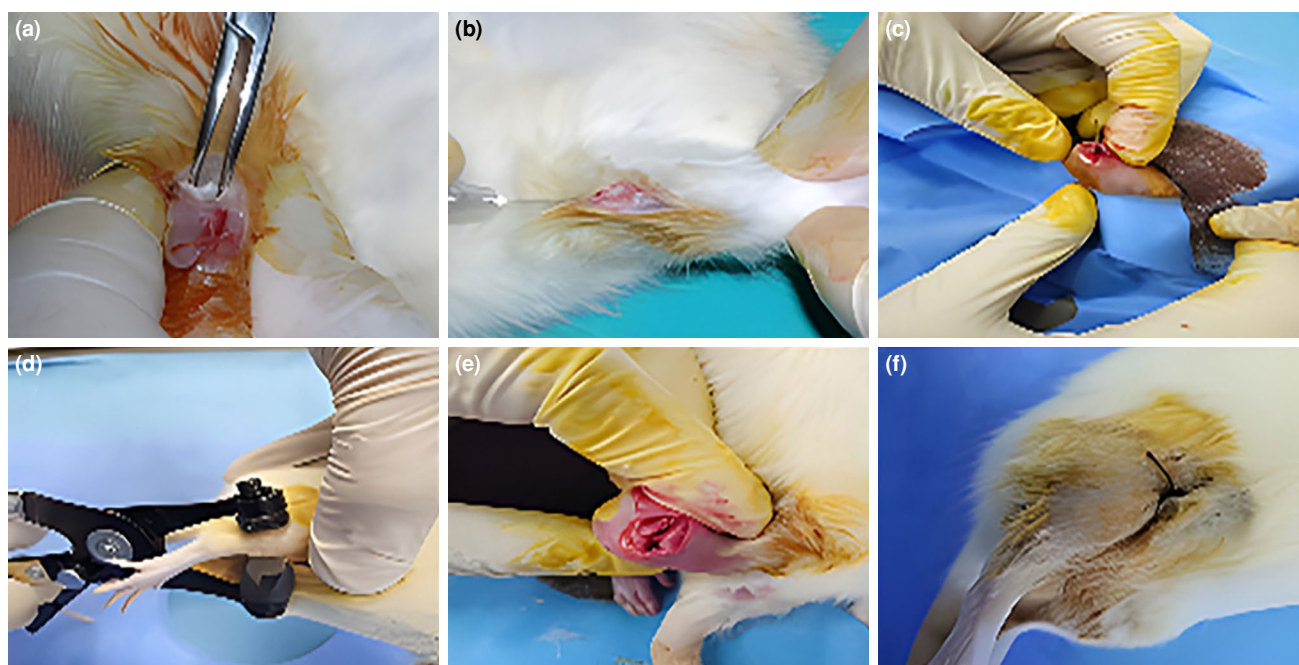


FIGURE 1. The experimental femoral fracture model in rats requires a surgical procedure which includes the following steps: (a) The anterior approach reveals femoral condyles after making a skin incision, (b) The surgeon prepares the intramedullary entry site in the femur, (c) The surgeon inserts a Kirschner wire (K-wire) to achieve internal stabilization, (d) The three-point bending forceps create a closed fracture through a custom-designed process, (e) The surgeon shortens the K-wire to stop skin irritation after surgery, (f) The surgeon uses sutures to seal the surgical area.

TABLE I
Experimental groups and study protocol

Group code	Group name	n	Fracture status	Vericiguat dose	Description
NC	Negative control	10	No	-	Healthy control
PC	Positive control	10	Yes	-	Fracture only
LDV-N	Low-dose vericiguat negative	10	No	3 mg/kg/day	Healthy + low dose
HDV-N	High-dose vericiguat negative	10	No	6 mg/kg/day	Healthy + high dose
LDV-P	Low-dose vericiguat positive	10	Yes	3 mg/kg/day	Fracture + low dose
HDV-P	High-dose vericiguat positive	10	Yes	6 mg/kg/day	Fracture + high dose

NC, Group 1; PC, Group 2; LDV-N, Group 3; HDV-N, Group 4; LDV-P, Group 5; HDV-P, Group 6.

perform the procedure while the K-wire tip was cut (Figure 1e) and the incision was closed with 4.0 silk suture (Ethicon, Johnson & Johnson, New Brunswick, NJ, USA) (Figure 1f). The physician confirmed fracture creation through both manual examination and X-ray images taken after the procedure. The first oral gavage administration of vericiguat started on the day of surgery followed by continuous administration until Day 28. The researchers chose the 28-day endpoint, as it matches the typical fracture healing period in rats which allows for full callus development.

Statistical analysis

Statistical analysis was performed using the IBM SPSS version 20.0 software (IBM Corp., Armonk, NY, USA). The Shapiro-Wilk test served to determine whether continuous variables followed a normal distribution pattern. The one-way analysis of variance (ANOVA) test was used for normally distributed data, while the Kruskal-Wallis test was used for data that did not follow normal distribution. The Tukey test served for post-hoc analyses after ANOVA when variances were homogeneous, while the Dunn's test with Bonferroni correction was used for non-parametric data after Kruskal-Wallis test. The Tamhane's T2 test was used when variances were not homogeneous. The study had no missing data, since all participants completed the study. The Lane-Sandhu criteria evaluated radiological scoring and the Huo scale was used for histopathological assessment. The researchers performed subgroup analyses independently for both fracture and non-fracture groups. The biomechanical test results were presented as maximum load capacity in Newton (N) and stiffness values in N/mm. The weights of animals were expressed in g, and drug doses in mg/kg/day (mg/kg/day). The numerical scoring system of 1-10 was used for histopathological evaluation

and a 0-4 scoring system was used for radiological assessment. Follow-up periods were reported on Days 7, 14, 28. The study reported *p* values alongside the analyzed groups and the statistical methods used for comparison. The results contained two decimal points for $p \geq 0.01$ (e.g., $p = 0.03$) and three decimal points for $p < 0.01$ (e.g., $p = 0.007$). *P* values below 0.001 appeared as $p < 0.001$ rather than their specific numerical values. The data were presented in mean \pm SD. A *p* value of < 0.05 was considered statistically significant with 95% confidence interval (CI).

RESULTS

The experimental protocol resulted in no animal losses and no serious complications were observed (Table I).

The Lane-Sandhu scoring system was used to evaluate fracture healing through radiographic assessments. Serial anteroposterior radiographs were used to evaluate the radiological healing process of all groups on Days 7, 14, and 28 (Figure 2). The NC group maintained normal bone architecture during the first week, but the fracture-induced groups showed no callus formation. The second week radiographic evaluations showed callus formation in the PC group and similar healing patterns in the vericiguat-treated groups. The mean values were 1.6 in the PC group, 1.6 in the LDV-P group, and 1.8 in the HDV-P group. The fourth week radiographic images showed complete bone union in the PC group and significant callus maturation in the LDV-P and HDV-P groups. All fracture groups showed significant improvement at the end of the fourth week, but no statistically significant differences were detected between the groups ($p = 0.811$ on Day 14; $p = 0.299$ on Day 28) (Table II).

The most notable findings of the study were revealed through the biomechanical test results.

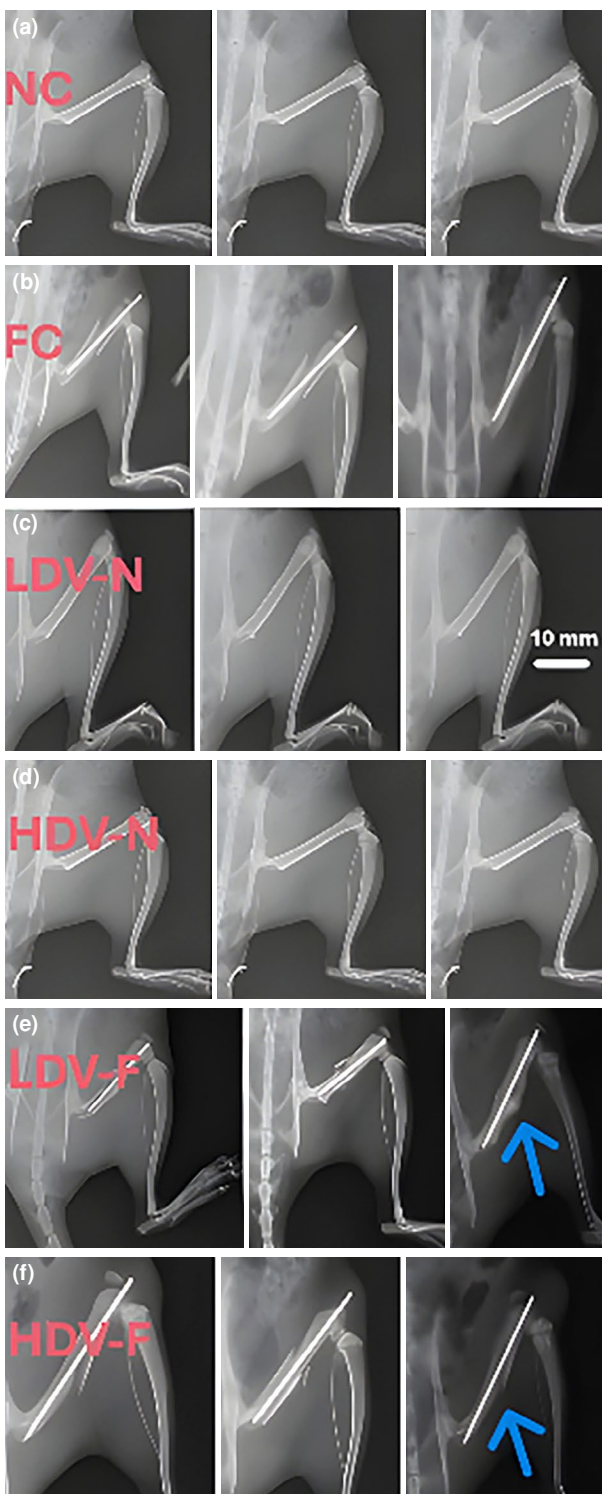


FIGURE 2. Radiological assessment of fracture healing at days 7, 14, and 28. Panels: (a) NC: Negative control; (b) FC: Fracture control; (c) LDV-N: Low-dose vericiguat negative (3 mg/kg); (d) HDV-N: High-dose vericiguat negative (6 mg/kg); (e) LDV-F: Low-dose vericiguat fracture (3 mg/kg); (f) HDV-F: High-dose vericiguat fracture (6 mg/kg).

Blue arrows indicate callus formation sites. Scale bar: 10 mm. NC, Group 1; FC, Group 2; LDV-N, Group 3; HDV-N, Group 4; LDV-F, Group 5; HDV-F, Group 6.

No adverse effects of vericiguat administration on bone structure were observed in the groups without fractures. The NC group showed an average load value of 115.32 N, the LDV-N group 106.87 N, and the HDV-N group 98.05 N. No statistically significant differences were found between these groups ($p = 0.795$). However, significantly different results were obtained in the fracture-induced groups. The HDV-P group showed the lowest mechanical resistance at 39.07 N compared to all other groups. This value was approximately half that of the PC group (88.75 N) and the LDV-P group (83.54 N) ($p = 0.003$) (Table III and Table IV).

The hardness values followed the same pattern as the other parameters. The HDV-P group had the lowest hardness value of 40.47 N/mm, while the LDV-P had higher values of 99.20 N/mm compared to the PC group (64.71 N/mm). These results were associated with dose-dependent effects of vericiguat (Table IV).

Histopathological examinations provided the most comprehensive evaluations of the study. In the callus formation assessment according to the Huo scale, the LDV-P group showed the highest value with an average score of 8.6. The group displayed sophisticated bone development through advanced ossification processes and mature bone tissue formation. The PC group maintained their tissue development at fibrous and cartilage stages with an average score of 2.6, while the HDV-P group achieved an intermediate level of improvement with a score of 4.4. The statistical analysis revealed significant differences between the groups ($p = 0.014$) (Table V).

The complication assessments produced the most remarkable findings. When evaluated for necrosis, no necrosis infiltration was observed in any of the groups without fractures or in the PC group. The HDV-P group showed necrosis in six out of 10 animals. Three of these animals showed mild necrosis and one had severe necrosis. The distribution of inflammation findings was associated with the necrosis findings. The HDV-P group showed severe inflammation in eight animals while the other groups had much milder findings (Table V). The histopathological imaging results supported these findings. The control groups maintained their normal bone architecture, but the PC group showed fibrous tissue formation and early cartilage callus development. The LDV-P group showed advanced callus formation and mature bone tissue and widespread ossification areas. The HDV-P group showed a disrupted

TABLE II
Radiographic evaluation of fracture groups using Lane-Sandhu scoring system

Groups	Day 7	Day 14	Day 28					<i>p</i>		
	Mean ± SD	Mean ± SD	Median	IQR	Min-Max	Mean ± SD	Median		IQR	Min-Max
PC	0 ± 0	1.6 ± 0.516	2	1-2	1-2	3.8 ± 0.422	4	3-4	3-4	0.299
LDV-P	0 ± 0	1.6 ± 0.699	1.5	1-2.25	1-3	3.5 ± 0.527	3.5	3-4	3-4	0.299
HDV-P	0 ± 0	1.8 ± 0.789	2	1-2.25	1-3	3.5 ± 0.527	3.5	3-4	3-4	0.299

SD, standard deviation; IQR, Interquartile range; PC, Group 2; LDV-P, Group 5; HDV-P, Group 6; Statistical comparisons between fracture groups were performed using the Kruskal-Wallis test.

TABLE III
Individual biomechanical test results at day 28

Groups	Rat No.	Load (N)	Deformation (mm)	Stiffness (N/mm)
NC	1	97.795	0.921	106.18
	2	80.229	0.955	84.01
	3	159.489	1.786	89.30
	4	168.586	1.354	124.51
	5	70.523	0.672	104.94
PC	1	103.814	0.988	105.07
	2	49.699	1.306	38.05
	3	100.403	3.121	32.17
	4	84.948	3.322	25.57
	5	104.879	0.855	122.67
LDV-N	1	137.797	2.405	57.30
	2	95.400	1.222	78.07
	3	127.240	1.888	67.39
	4	102.501	1.220	84.02
	5	71.433	0.804	88.85
HDV-N	1	170.186	1.821	93.46
	2	113.690	1.970	57.71
	3	66.999	0.604	110.93
	4	70.801	0.903	78.41
	5	68.590	0.587	116.85
LDV-P	1	85.550	1.037	82.50
	2	83.857	1.336	62.77
	3	117.956	0.772	152.79
	4	76.992	0.554	138.97
	5	53.352	0.905	58.95
HDV-P	1	33.894	0.904	37.49
	2	53.973	1.988	27.15
	3	30.730	0.586	52.44
	4	45.865	0.689	66.57
	5	30.903	1.653	18.70

NC, Group 1; PC, Group 2; LDV-N, Group 3; HDV-N, Group 4; LDV-P, Group 5; HDV-P, Group 6.

TABLE IV
Biomechanical test results - group means and statistical comparisons

Groups	Load (N)		Stiffness (N/mm)			Deformation (mm)			Mean ± SD	Median	Min-Max
	n	Mean ± SD	Median	Min-Max	Mean ± SD	Median	Min-Max				
Non-fracture groups											
NC	5	115.32 ± 45.64	97.80	70.52-168.59	101.79 ± 15.95	104.94	84.01-124.51	1.14 ± 0.47			0.92
LDV-N	5	106.87 ± 26.35	102.50	71.43-137.80	75.12 ± 12.78	78.07	57.30-88.85	1.51 ± 0.67			1.22
HDV-N	5	98.05 ± 44.79	70.80	66.99-170.19	91.47 ± 24.17	93.46	57.71-116.85	1.18 ± 0.66			0.90
Fracture groups											
PC	5	88.75 ± 23.25	100.40	49.70-104.88	64.71 ± 45.52	38.05	25.57-122.67	2.00 ± 1.23			0.99
LDV-P	5	83.54 ± 23.15	83.86	53.35-117.96	99.20 ± 43.82	82.50	58.95-152.79**	0.92 ± 0.32			0.91
HDV-P	5	39.07 ± 10.38	33.89	30.73-53.97	40.47 ± 19.27	37.49	18.70-66.57	1.16 ± 0.60			0.90

SD, standard deviation; NC, Group 1; PC, Group 2; LDV-N, Group 3; HDV-N, Group 4; LDV-P, Group 5; HDV-P, Group 6; Statistical analyses: Non-fracture groups: One-way ANOVA, F = 0.234, p = 0.795 (Load); F = 2.706, p = 0.107 (Stiffness). Fracture groups: One-way ANOVA, F = 9.442, p = 0.003 (Load); F = 2.994, p = 0.088 (Stiffness). Post-hoc (Tukey test): PK-YVP (p = 0.012), DVP-YVP (p = 0.008). **Potential outlier identified in DVP group (152.79 N/mm).

TABLE V
Histopathological evaluation and complications at Day 28

Groups	Callus formation (Huo Scale 1-10)			Necrosis distribution†			Inflammation distribution‡				
	Mean ± SD	Median	Min-Max	None(0)	Mild(1)	Moderate(2)	Severe(3)	None(0)	Mild(1)	Moderate(2)	Severe(3)
NC	-	-	-	10/10	0/10	0/10	0/10	10/10	0/10	0/10	0/10
PC	2.6 ± 0.548	3	2-3	10/10	0/10	0/10	0/10	7/10	1/10	2/10	0/10
LDV-N	-	-	-	10/10	0/10	0/10	0/10	10/10	0/10	0/10	0/10
HDV-N	-	-	-	10/10	0/10	0/10	0/10	6/10	0/10	4/10	0/10
LDV-P	8.6 ± 1.14	9	7-10	10/10	0/10	0/10	0/10	7/10	3/10	0/10	0/10
HDV-P	4.4 ± 2.881	3	2-8	6/10	3/10	0/10	1/10	1/10	1/10	0/10	8/10

SD, standard deviation; NC, Group 1; PC, Group 2; LDV-N, Group 3; HDV-N, Group 4; LDV-P, Group 5; HDV-P, Group 6; Callus formation statistics: Kruskal-Wallis test, $\chi^2 = 8.61$, p = 0.014. Post-hoc (Dunn test): PK-DVP (p = 0.009). †, necrosis grading; 0, absent; 1, focal necrosis (< 10% of tissue); 2, multifocal necrosis (10-30%); 3, diffuse necrosis (> 30%); ‡, inflammation grading; 0, absent; 1, mild (1-10 inflammatory cells/HPF); 2, moderate (11-50 cells/HPF); 3, severe (> 50 cells/HPF).



FIGURE 3. The H&E staining at $\times 100$ magnification shows control and non-fracture groups from day 28. The images show the following: (a) NC: The negative control shows typical trabecular bone structure; (b) FC: The fracture control shows fibrous tissue and early cartilaginous callus formation at the fracture location (Huo score: 2.6 ± 0.548); (c) LDV-N: The low-dose vericiguat negative group received 3 mg/kg without any bone structure changes. Scale bar: 100 μm .

NC, Group 1; FC, Group 2; LDV-N, Group 3.

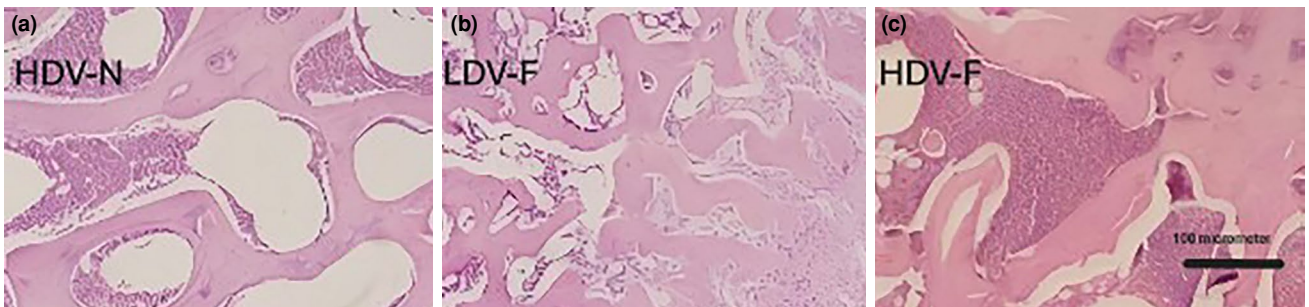


FIGURE 4. The histopathological assessment of vericiguat-treated groups at day 28 used H&E staining to examine tissue samples at $\times 100$ magnification. The images show three groups of bone tissue: (a) HDV-N: High-dose vericiguat negative (6 mg/kg) with normal bone structure; (b) LDV-F: Low-dose vericiguat fracture (3 mg/kg) shows complete callus development and bone maturation (Huo score: 8.6 ± 1.14); (c) HDV-F: High-dose vericiguat fracture (6 mg/kg) shows tissue fibrosis and dead tissue and inflammatory cells that block the healing process (Huo score: 4.4 ± 2.88). Scale bar: 100 μm .

HDV-N, Group 4; LDV-F, Group 5; HDV-F, Group 6.

healing process with fibrous tissue infiltration and necrotic areas and inflammatory cell accumulation (Figures 3 and 4).

Vericiguat was found to be associated with dose-dependent dual effects on bone fracture healing. The drug was associated with enhanced bone healing at low doses, yet was associated with severe adverse effects and impaired healing at high doses.

DISCUSSION

In the present study, we assessed the healing effects of vericiguat at various concentrations on rat femur fractures through clinical and radiological and biomechanical and histopathological assessments. Our study results showed that vericiguat produced dose-dependent effects which either promote or hinder fracture healing processes. The

histopathological results from low-dose vericiguat (3 mg/kg) administration indicated bone healing support, while high-dose (6 mg/kg) administration resulted in tissue-level necrosis and inflammation while decreasing biomechanical performance.

To the best of our knowledge, this study represents the first study of vericiguat effects on fracture healing. Previous research has investigated sGC agonists for bone metabolism, although these compounds produced different results based on the administered amount.^[4,10] The closed fracture model used in our study was based on protocols developed by Jackson et al. in 1970 and improved by Bonnarens and Einborn in 1984.^[13] The closed fracture model was selected, as it can reduce the occurrence of delayed union and infection risks and non-union complications that open osteotomy techniques present. The literature reveals that

using an intramedullary K-wire improves surgical stability^[14] and our study adopted this method to increase methodological reliability.

The selection of female Wistar-Albino rats as experimental animals is consistent with similar studies in the literature.^[15] The choice of this approach stems from its high availability and rapid adaptation capabilities and resistance to infections and low cost. The selection of female animals who have not mated before remains essential, since it reduces experimental variability and prevents hormonal influences on study outcomes. Our study achieved complete animal survival because of strict sterilization protocols and professional team collaboration.

Sun et al.^[6] performed an *in vitro* study which showed vericiguat affects osteoclast differentiation through dose-dependent mechanisms. The effects of vericiguat on osteoclast differentiation follow an inverse pattern according to concentration: low doses between 100 nM and 1 μ M enhance differentiation, while high doses between 4 μ M and 8 μ M block this process. This effect occurs via the VASP/inhibitor of kappa B alpha (I κ B- α)/NF- κ B signaling pathway. The positive histopathological findings observed in the low-dose group and the necrosis and inflammation findings in the high-dose group in our study appear consistent with these molecular mechanisms.

The low-dose administration of vericiguat was associated with faster callus development and produced superior histopathological scores, indicating an optimal osteoclast activity for bone remodeling. The high-dose group experienced negative effects on fracture healing, as excessive osteoclast suppression was associated with bone resorption inhibition and delayed bone remodeling. The high-dose vericiguat group (39.07 N) showed mechanical resistance values that were approximately half of the positive control group (88.75 N) and the low-dose group (83.54 N). The significant drop in bone quality became evident through this substantial reduction. The hardness measurements followed the same pattern as the mechanical resistance results, as the high-dose group produced the lowest values at 40.47 N/mm.

The research by Homer et al.^[10] showed that sGC agonists at toxic doses between 25 mg/kg and 500 mg/kg increased osteoclastic bone resorption and caused bone marrow tissue death. The researchers observed that high doses of the compound triggered osteoclastic activation and caused both cortical and trabecular bone resorption

and increased bone porosity. The study results confirm the negative effects of high-dose vericiguat administration in our research. The necrosis and inflammation found in callus tissue indicates that excessive bone resorption is associated with weakened biomechanical properties of the tissue.

The clinical value of our dosing approach needs thorough evaluation for proper assessment. The Vericiguat Global Study in Subjects with Heart Chronic Heart Failure with Reduced Ejection Fraction (VICTORIA) trial determined 10 mg/day as the safe human dosage which equals 0.14 mg/kg for humans and 0.86 mg/kg in rat equivalents.^[8] The experimental doses of 3 to 6 mg/kg exceed the clinical dose by three to seven times which might lead to toxic effects at higher concentrations. The sGC activation in bone metabolism shows a restricted range between effective and toxic levels.

Tao and Shen^[16] demonstrated in their study that vericiguat combined with β -tricalcium phosphate enhanced osteogenic activity in ovariectomized rats. The current study showed that a 5-mg dose produced better results than the high-dose group in our study, although the aforementioned study produced negative results. The main factors behind this disagreement stem from β -tricalcium phosphate supplementation synergy and the different study durations (12 weeks *vs.* 4 weeks) and natural differences between osteoporotic bone defects and healthy bone fractures. The positive findings from Tao and Shen's study^[17] using 10 mg/kg vericiguat on elderly (24-month-old) rats indicate that both age and oxidative stress levels affect how vericiguat works. The age difference between our eight-week-old rats and the study subjects and the varying follow-up periods in our research explain the observed discrepancies in results.

Furthermore, our study reveals a major inconsistency between the results obtained through histopathological examination and radiological imaging. Despite the histopathological evaluation according to the Huo scale showing a significantly higher quality of improvement (average score of 8.6) in the low-dose vericiguat group compared to the positive control group (score of 2.6), no significant difference was detected between the groups in the Lane-Sandhu radiological scoring. The literature supports this inconsistency, as Zhu et al.^[18] demonstrated that the Lane-Sandhu X-ray scoring system failed to detect treatment group differences in rabbit radius models especially during early bone quality changes. Menger et al.^[19] found that radiographic scores failed to match

histopathological results in elderly mice while conventional radiography proved insufficient for detecting small bone tissue quality changes.

The lack of statistically significant differences between groups in radiological evaluations using the Lane-Sandhu scoring system suggests that this method may be insufficient for detecting subtle changes in bone quality. Previous studies have raised doubts about conventional radiography sensitivity when it comes to detecting initial bone quality alterations.^[18,19] The main study limitation arises from the absence of advanced imaging tools including micro-computed tomography (micro-CT). Future research needs to study callus development through more precise imaging techniques.

The biomechanical stiffness values (99.20 N/mm) in the low-dose group exceeded those of the positive control group (64.71 N/mm) by 53%. The superior results were associated with both successful healing and the creation of a callus structure that exceeded normal bone strength. Menger et al.^[19] also reported that bending stiffness values paralleled histopathological findings and serve as the most reliable indicator of bone quality. The mechanical properties of collagen-based hydrogels directly influence the formation of advanced callus and mature bone tissue according to De Pace et al.^[20] The histopathological examination revealed advanced callus formation and mature bone tissue formation and widespread ossification areas which establish the morphological basis for this mechanical superiority.

The findings observed in the high-dose vericiguat group indicate that changes at the micro and macro levels in bone healing may develop with different kinetics and that overdose is associated with serious toxicity. The histopathological score (4.4) in this group exceeded the positive control group (2.6), yet the biomechanical test results (39.07 N) were extremely low suggesting that callus formation does not always lead to functional improvement. The literature supports this paradox as Karasu et al.^[21] found histopathological improvement alongside substantial wound healing impairment in patients receiving high-dose methotrexate treatment. In the aforementioned study, the severe (+++) necrotic area reported on Day 7 in the high-dose group is consistent with our findings.

The quality of callus tissue was associated with substantial impairment by necrosis ($n = 6/10$) and widespread inflammation (severe $n = 8$). The results of Kyllönen et al.^[22] in their studies

with bone morphogenetic protein-7 (BMP-7) were similar, showing that excessive doses of BMP-7 are detrimental to bone healing, with no fusion observed at doses of 10 to 30 μg , while bone fusion was only observed at a dose of 90 μg (three times the normal dose). These results highlight the need for an appropriate dose range for bone healing.

The performance in healthy bones showed a dose-dependent decline from NK: 115.32 N to DVN: 106.87 N to YVN: 98.05 N. Although this gradual decline pattern did not reach statistical significance, it indicates potential risks associated with long-term use of vericiguat. Hedayatzadeh Razavi et al.^[23] also emphasized that callus hardness should reflect physiological callus growth and that optimal mechanical performance was directly related to bone quality. The research indicates that vericiguat treatment for fracture healing needs precise dose adjustments, as its therapeutic benefits exist within a very limited range.

The research by Singh et al.^[24] demonstrated that nitroglycerin as a NO donor produced effects depending on the frequency of administration. The research showed that daily administration of low-dose nitroglycerin discontinued bone mineral density decline, while multiple daily doses of the same amount became ineffective. The research demonstrates that the NO-sGC-cGMP pathway requires precise control, since optimal dosing represents a critical factor. In an *in vitro* study by Abnos et al.,^[25] NO supported osteoblast proliferation at low concentrations, but had the opposite effect at high concentrations. The biphasic effect pattern matches the dose-dependent results from our study which demonstrates why dose optimization is needed to understand the role of vericiguat in bone healing.

The study by Joshua et al.^[4] showed that the NO-independent sGC activator cinaciguat enhanced bone mineral density while promoting osteoblast function in osteoporotic mice. The research results indicate that sGC activation may have beneficial effects on bone health when appropriately dosed. The positive results of low-dose vericiguat in our study suggest that this drug may support fracture healing at optimized doses.

Nonetheless, this study has certain limitations. First, the study failed to measure vericiguat levels in serum and tissue which makes it difficult to link drug amounts to the observed results. Second, the study lacked micro-CT imaging which prevented researchers from performing

detailed three-dimensional assessments of callus microstructure. Third, we were unable to evaluate systemic toxicity indicators and potential secondary effects of vericiguat on body organs. The four-week observation period might not be enough to detect long-term effects or late complications that could develop. Fourth, estrous cycle variations were not controlled, which may have influenced the study outcomes. Finally, the study did not include measurements of bone turnover biomarkers including alkaline phosphatase (ALP) and tartrate-resistant acid phosphatase (TRAP) and inflammatory cytokines to understand the mechanisms behind the observed results.

On the other hand, our study benefits from a controlled experimental setting and a multi-group comparative design and a multidisciplinary evaluation approach (radiological, biomechanical, histopathological). The research presents the first investigation of vericiguat effects on bone fracture recovery which generates essential findings for this developing medical field. Future research needs to include biochemical tests and extended observation times and sophisticated imaging techniques and optimized treatment schedules to evaluate the full potential of vericiguat for fracture treatment.^[26]

In conclusion, our study results suggest that sGC activators show promise for fracture healing treatment when used at specific concentrations, but their therapeutic range remains limited and their toxic effects at high doses need careful consideration. The research requires clinical and longitudinal follow-up studies to confirm these initial results and develop proper treatment methods.

Data Sharing Statement: The data that support the findings of this study are available from the corresponding author upon reasonable request.

Author Contributions: A.D., B.K.: Idea/concept, design, writing the article, critical review; A.D., M.Ç.E.: Control/supervision; B.K., F.Y.H.: Data collection and/or processing; M.Ç.E., A.D.: Analysis and/or interpretation; A.D., A.D.: Literature review; M.Ç.E., A.D.: References and fundings; A.D., F.Y.H.: Materials; F.Y.H., A.D.: Other.

Conflict of Interest: The authors declared no conflicts of interest with respect to the authorship and/or publication of this article.

Funding: This research was supported by Atatürk University Scientific Research Projects as a project code TTU-2023-13018.

AI Disclosure: The authors declare that artificial intelligence (AI) tools were not used, or were used solely for language editing, and had no role in data analysis,

interpretation, or the formulation of conclusions. All scientific content, data interpretation, and conclusions are the sole responsibility of the authors. The authors further confirm that AI tools were not used to generate, fabricate, or 'hallucinate' references, and that all references have been carefully verified for accuracy.

REFERENCES

1. Açıan AE, Aydın ME, Bulmuş Ö, Özcan E, Karakılıç A, Turan G, et al. The effects of gabapentin and pregabalin on fracture healing: A histological, radiological, and biomechanical analysis. *Jt Dis Relat Surg* 2025;36:200-9. doi: 10.52312/jdrs.2025.2042.
2. Erener T, Ceritoğlu KU, Aktekin CN, Dalgıç AD, Keskin D, Geneci F, et al. Investigation of the effect of ghrelin on bone fracture healing in rats. *Clin Exp Pharmacol Physiol* 2021;48:1382-90. doi: 10.1111/1440-1681.13544.
3. Gogna S, Maxwell J, Policastro AJ, Latifi R. Nutrition support in elderly patients undergoing surgery. In: Latifi R, editor. *Surgical decision making in geriatrics*. Cham: Springer; 2020. p. 103-17. doi: 10.1007/978-3-030-47963-3_8.
4. Joshua J, Schwaerzer GK, Kalyanaraman H, Cory E, Sah RL, Li M, et al. Soluble guanylate cyclase as a novel treatment target for osteoporosis. *Endocrinology* 2014;155:4720-30. doi: 10.1210/en.2014-1343.
5. Korkmaz Y, Puladi B, Galler K, Kämmerer PW, Schröder A, Gözl L, et al. Inflammation in the human periodontium induces downregulation of the $\alpha 1$ - and $\beta 1$ -subunits of the sGC in cementoclasts. *Int J Mol Sci* 2021;22:539. doi: 10.3390/ijms22020539.
6. Sun K, Kong F, Lin F, Li F, Sun J, Ren C, et al. Vericiguat modulates osteoclast differentiation and bone resorption via a balance between VASP and NF- κ B pathways. *Mediators Inflamm* 2022;2022:1625290. doi: 10.1155/2022/1625290.
7. Wisanwattana W, Wongkrajang K, Cao DY, Shi XK, Zhang ZH, Zhou ZY, et al. Inhibition of phosphodiesterase 5 promotes the aromatase-mediated estrogen biosynthesis in osteoblastic cells by activation of cGMP/PKG/SHP2 pathway. *Front Endocrinol (Lausanne)* 2021;12:636784. doi: 10.3389/fendo.2021.636784.
8. Armstrong PW, Roessig L, Patel MJ, Anstrom KJ, Butler J, Voors AA, et al. A multicenter, randomized, double-blind, placebo-controlled trial of the efficacy and safety of the oral soluble guanylate cyclase stimulator: The VICTORIA Trial. *JACC Heart Fail* 2018;6:96-104. doi: 10.1016/j.jchf.2017.08.013.
9. Percie du Sert N, Hurst V, Ahluwalia A, Alam S, Avey MT, Baker M, et al. The ARRIVE guidelines 2.0: Updated guidelines for reporting animal research. *PLoS Biol* 2020;18:e3000410. doi: 10.1371/journal.pbio.3000410.
10. Homer BL, Morton D, Bagi CM, Warneke JA, Andresen CJ, Whiteley LO, et al. Oral administration of soluble guanylate cyclase agonists to rats results in osteoclastic bone resorption and remodeling with new bone formation in the appendicular and axial skeleton. *Toxicol Pathol* 2015;43:411-23. doi: 10.1177/0192623314546559.
11. Zhang Y, Shen L, Mao Z, Wang N, Wang X, Huang X, et al. Icaritin enhances bone repair in rabbits with bone infection during post-infection treatment and prevents inhibition of

- osteoblasts by vancomycin. *Front Pharmacol* 2017;8:784. doi: 10.3389/fphar.2017.00784.
12. Huo MH, Troiano NW, Pelker RR, Gundberg CM, Friedlaender GE. The influence of ibuprofen on fracture repair: Biomechanical, biochemical, histologic, and histomorphometric parameters in rats. *J Orthop Res* 1991;9:383-90. doi: 10.1002/jor.1100090310.
 13. Handool KO, Ibrahim SM, Kaka U, Omar MA, Abu J, Yusoff MSM, et al. Optimization of a closed rat tibial fracture model. *J Exp Orthop* 2018;5:13. doi: 10.1186/s40634-018-0128-6.
 14. Ahmad S, Gupta T, Ansari S, Jain A, Barik S, Singh V. Intramedullary crossed K-wire fixation for the hand fractures is a useful treatment modality: A prospective observational study. *Strategies Trauma Limb Reconstr* 2022;17:74-80. doi: 10.5005/jp-journals-10080-1556.
 15. Prodinge PM, Bürklein D, Foehr P, Kreutzer K, Pilge H, Schmitt A, et al. Improving results in rat fracture models: Enhancing the efficacy of biomechanical testing by a modification of the experimental setup. *BMC Musculoskelet Disord* 2018;19:243. doi: 10.1186/s12891-018-2155-y.
 16. Tao ZS, Shen CL. Favorable osteogenic activity of vericiguat doped in β -tricalcium phosphate: In vitro and in vivo studies. *J Biomater Appl* 2024;38:1073-86. doi: 10.1177/08853282241245543.
 17. Tao ZS, Shen CL. Guanylate cyclase promotes osseointegration by inhibiting oxidative stress and inflammation in aged rats with iron overload. *Bone Joint Res* 2024;13:427-40. doi: 10.1302/2046-3758.139.BJR-2023-0396.R3.
 18. Zhu J, Wang F, Yan L, Wang J, Wu M, Hu R, et al. Negative pressure wound therapy enhances bone regeneration compared with conventional therapy in a rabbit radius gap-healing model. *Exp Ther Med* 2021;21:474. doi: 10.3892/etm.2021.9905.
 19. Menger MM, Manuschewski R, Ehnert S, Rollmann MF, Maisenbacher TC, Tobias AL, et al. Radiographic, biomechanical and histological characterization of femoral fracture healing in aged CD-1 mice. *Bioengineering (Basel)* 2023;10:275. doi: 10.3390/bioengineering10020275.
 20. De Pace R, Molinari S, Mazzoni E, Perale G. Bone regeneration: A review of current treatment strategies. *J Clin Med* 2025;14:1838. doi: 10.3390/jcm14061838.
 21. Karasu A, Kuşçu Y, Kayıkci C, Yıldırım S, Kuşçu O, Kiliçlioğlu M. Effect of low- and high-dose methotrexate on wound healing in rats. *Acta Cir Bras* 2025;40:e403225. doi: 10.1590/acb403225.
 22. Kyllönen L, D'Este M, Alini M, Eglin D. Local drug delivery for enhancing fracture healing in osteoporotic bone. *Acta Biomater* 2015;11:412-34. doi: 10.1016/j.actbio.2014.09.006.
 23. Hedayatzadeh Razavi A, Nafisi N, Ghiasi MS, Oftadeh R, Hanna P, Lechtig A, et al. A computational model that integrates unrestricted callus growth, mechanobiology, and angiogenesis can predict bone healing in rodents. *Sci Rep* 2024;14:29826. doi: 10.1038/s41598-024-80502-2.
 24. Singh S, Sharma P, Dixit D, Mandal MB. Role of nitric oxide in determination of large intestinal contractility in neonatal rats. *Indian J Physiol Pharmacol* 2024;68:9-17. doi: 10.25259/IJPP_374_2023.
 25. Abnos MH, Sargolzaei J, Maleklou M. Exogenous nitric oxide up-regulates the Runx2 via Bmp7 overexpression to increase the osteoblast matrix production in vitro. *Avicenna J Med Biochem* 2022;10:58-64. doi: 10.34172/ajmb.2022.08.
 26. Calavul A, Özalp B, Menekşe S. Efecto de los anticonceptivos orales combinados en la cirugía de colgajo en el modelo de rata hembra. *Rev Cient Fac Cienc Vet* 2025;35:10. doi: 10.52973/rcfcv-e35611.